

Electric-dipole spin resonance of localized electron states at dislocation dipoles in undeformed oxygen-containing silicon

V. M. Babich, N. P. Baran, A. A. Bugai, A. A. Konchits, and B. D. Shanina

Institute of Semiconductors, Academy of Sciences of the Ukrainian SSR, Kiev

(Submitted 27 December 1987)

Zh. Eksp. Teor. Fiz. **94**, 319–330 (August 1988)

An electric-dipole spin resonance (EDSR) of new local centers at dislocation dipoles, formed as a result of prolonged annealing of undeformed silicon, was observed for the first time and investigated. At low temperatures (1.7–40 K) such undeformed silicon samples exhibited considerable microwave conductivity, the behavior of which was correlated with that of EDSR of new (Si-2K and Si-3K) centers. The intensity and profile of the EDSR signals due to these centers depended on the intensity and orientation of the E_1 component of the microwave field and the absorption lines were in the form of asymmetric dispersion curves. Both the resonant and the microwave conductivity disappeared (reversibly) as a result of interband illumination and irreversibly as a result of ultrasonic excitation of considerable amplitude, electron or gamma-ray bombardment, or annealing at $T \geq 1150$ K. The Rashba and Sheka theory of the EDSR was modified for the case of local dislocation centers. A theory was developed of the profile of the EDSR lines, which accounts completely for the experimental results.

1. INTRODUCTION

There have been many investigations of the electron states of dislocations in silicon subjected to plastic deformation.¹⁻⁹ One of the most informative methods for investigating these states is the ESR technique. However, usually the ESR spectra of dislocation centers are poorly resolved and to extract information from these spectra requires analysis of the dynamic behavior of spectral lines.⁹ This is a consequence of a weak manifestation of the “individual” characteristics of electron states in different parts of free dislocations. “Individualization” of electron states achieved by creation of distorted dislocations pinned by impurities and of partial dislocations representing components of Frank, Bloch, and other stacking faults, makes it possible to acquire more information on the properties of electrons localized at dislocations.

As shown in Refs. 10 and 11, such stacking faults appear in heat-treated silicon with high oxygen concentrations. Annealing of samples of this material in the range 700–1100 K creates paramagnetic defects of different types, including thermal donors.¹⁰ The interest in these donors is due to the attempt to identify the nature of the states, which is not fully understood at present, and also due to the fact that they are electrically active and thus influence the characteristics of semiconductor structures. It is shown in Ref. 11 that type II thermal donors (TD-II) which appear as a result of annealing at $T_{\text{ann}} \approx 900$ K are related to the localization of electrons and fluctuations of the crystal potential due to the presence of oxygen clusters.

New properties of these crystals revealed as a result of prolonged annealing were reported in Ref. 12. At low temperatures such crystals exhibit considerable microwave conductivity the presence of which is correlated with the appearance of paramagnetic centers that have anomalous spin resonance characteristics. It is postulated that this unusual behavior of the paramagnetic centers is associated with the appearance of a combined resonance of electrons in a quasi-one-dimensional system by analogy with that observed in plastically deformed silicon.⁸

The present paper reports a detailed investigation of the properties of these states. It was found that the observed spin resonance signals were associated with the new class of paramagnetic centers (which we by Si-2K, Si-3K, and Si-4K) of dislocation origin. These centers were located at cores of dislocation dipoles formed in silicon containing oxygen as a result of prolonged annealing. We found that the characteristics of these centers were closely related to the physical characteristics of dislocation dipoles with which they were associated. Anomalous properties of the spin resonance signals of Si-2K and Si-3K centers were explained using the theory of electric-dipole spin resonance (EDSR)¹³ modified to the case of local dislocation centers. A theory of the EDSR line profile was developed and it was found that the observed EDSR lines were a mixture of absorption and dispersion signals, with relative contributions depending on the orientation of a sample relative to the E_1 component of a microwave field and to a static magnetic field H_0 . The results of this theory were compared quantitatively with the experimental data.

2. EXPERIMENTAL METHOD

We used electrophysical (Hall effect, electrical conductivity) and ESR methods to study samples of silicon grown by the Czochralski method which were annealed at $T = 870$ – 1070 K. The electrophysical measurements were made under dc conditions. The ESR spectra were recorded using a Varian E-12 spectrometer ($\nu_{\text{micr}} \approx 9.5$ GHz) and a superheterodyne spectrometer ($\nu_{\text{micr}} \approx 9.4$ GHz) at temperatures in the range 1.7–40 K. Samples were subjected to illumination from an incandescent lamp of 150 W power using a light pipe or illuminating a sample directly through a quartz window in a cryostat.

We investigated samples of silicon which initially exhibited *n*- and *p*-type conduction and which contained phosphorus [$(0.15$ – $1) \times 10^{15}$ cm⁻³ or boron [$(0.5$ – $5) \times 10^{15}$ cm⁻³] as dopants and also oxygen [$(4$ – $10) \times 10^{17}$ cm⁻³] and carbon [$(0.15$ – $8) \times 10^{17}$ cm⁻³] as accidental impurities (the oxygen and carbon concentrations were deduced from

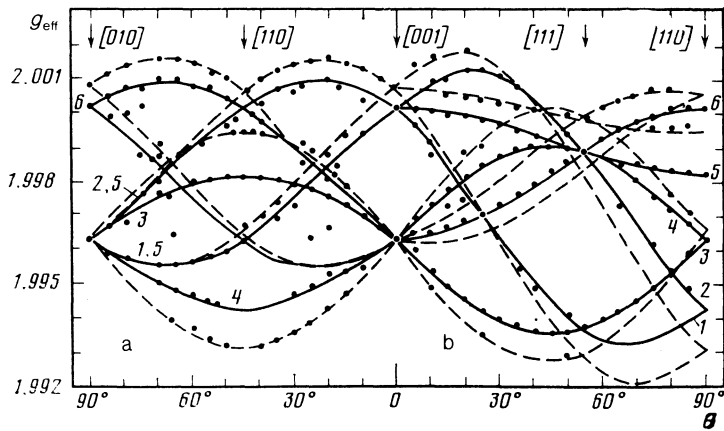


FIG. 1. Angular dependence of the resonance fields obtained associated with rotation of \mathbf{H}_0 in the following crystallographic planes: a) (100); b) (110). The points are the experimental results. The continuous (Si-2K) and dashed (Si-3K) lines are theoretical. Numbers 1–6 label (in an arbitrary manner) the curves representing the Si-2K centers localized at dislocation dipoles with axes oriented in different ways.

the infrared absorption spectra). In the main series of experiments our samples were annealed at $T = 920$ K (for 20–200 h) in air with or without a preliminary annealing at $T = 720$ K (20–100 h). The preliminary annealing accelerated the rate of formation of thermal defects.

3. EXPERIMENTAL RESULTS

Irrespective of the initial type of conduction, the annealed samples always contained TD-II thermal donors^{10,11} (there is as yet no standard terminology for these donors and they are called “new donors,” “oxygen donors,” etc.), which were detected by electrical and ESR measurements. These TD-II donors formed, below the bottom of the conduction band E_c a quasicontinuous spectrum of levels in the band gap of silicon with $E_i = E_c - 0.01\text{--}0.3$ eV (fluctuation states),¹⁴ which corresponded to an ESR spectrum consisting of a single asymmetric line with an anisotropic g factor (1.9984–1.9998) depending on the duration of annealing.¹¹

In addition to the TD-II donors, we found that prolonged annealing of samples with low carbon concentrations generated new Si-2K, Si-3K, and Si-4K centers (which we shall refer to simply as the 2, 3, and 4 centers). They gave rise to a complex spin resonance spectrum in darkness: this spectrum consisted of over 20 narrow ($\Delta H \approx 0.03$ mT) lines in static magnetic fields \mathbf{H}_0 of arbitrary orientation. The angular dependences of the spectra are plotted in Fig. 1.

The characteristics of the spin resonance of the 2 and 3 centers were distinguished by a number of anomalous properties. Under normal conditions for the observation of the ESR signal, when the samples (of $\approx 2 \times 2 \times 10$ mm dimensions) were placed at an antinode of the \mathbf{H}_1 component of a

microwave field in a cylindrical resonator of the TE_{011} type, the profile and intensity of the spin resonance lines of these centers depended on the orientation of a sample relative to \mathbf{H}_0 . For this reason we plotted only a few experimental points on top of some of the theoretical curves in Fig. 1.

Displacement of a sample to an antinode of the \mathbf{E}_1 component of the microwave field increased the intensities of the spin resonance lines of the 2 and 3 centers, whereas the intensity of the usual ESR spectrum of the TD-II centers present in a sample fell strongly because of a reduction in \mathbf{H}_1 . The intensities and the profiles of the spin resonance lines of these centers exhibited a dependence on the orientation of \mathbf{E}_1 . Figure 2 shows a typical profile of the absorption lines belonging to the spectrum of the center 2, which were obtained for two orientations \mathbf{E}_1 recorded with an oscilloscope directly from the wide-band output of the superheterodyne spectrometer tuned so as to determine; the imaginary part χ'' of the paramagnetic susceptibility $\chi = \chi' - i\chi''$. Clearly, the intensity of the low-field part of the spectrum in the $\mathbf{E}_1 \parallel [110]$ and $\mathbf{H}_0 \parallel [100]$ cases was almost an order of magnitude higher than the intensity in the $\mathbf{E}_1 \parallel \mathbf{H}_0 \parallel [100]$ case. When \mathbf{H}_0 was rotated in the (110) plane, the intensity of the lines 1 and 2 (Fig. 1) of the center 2 was always less than of the other lines of this spectrum. At low microwave powers $P_{\text{micr}} < 10^{-6}$ W the amplitude of the lines in the spectrum (proportional to $P_{\text{abs}}^{1/2}$) increased on increase in \mathbf{E}_1 in accordance with a law which was nearly linear and for $P_{\text{micr}} \approx 10^{-4}$ W the spectra of the centers 2 and 3 became saturated (Fig. 3).

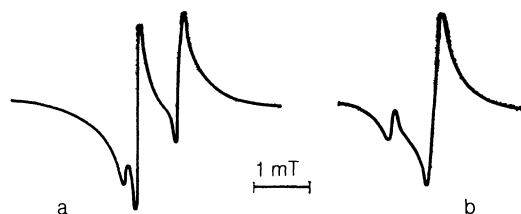


FIG. 2. Profiles of absorption lines of the Si-2K centers (taken from the screen of an oscilloscope): a) $\mathbf{E}_1 \parallel [110]$, $\mathbf{H}_0 \parallel [100]$ (the extreme line on the left belongs to the spectrum of Si-3K); b) $\mathbf{E}_1 \parallel \mathbf{H}_0 \parallel [100]$. $T = 4.2$ K and $P_{\text{micr}} \approx 10^{-5}$ W.

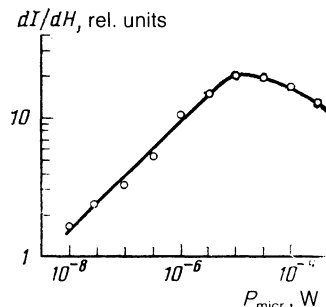


FIG. 3. Intensity of the spectrum of the Si-2K centers as a function of P_{micr} obtained using a superheterodyne spectrometer with $f_{\text{mod}} = 37$ Hz; $T = 4.2$ K, $\mathbf{H}_0 \parallel [100]$, $\mathbf{E}_1 \parallel [110]$.

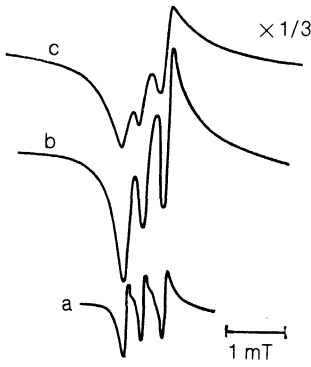


FIG. 4. Form of the EDSR spectrum of the Si-2K centers observed for different values of P_{micr} ; $T = 4.2$ K, $\mathbf{H}_0 \parallel [110]$; a), b), c) $P_{\text{micr}} 10^{-6}$, 10^{-5} and 10^{-4} W, respectively.

A special feature of the observed spectrum should be stressed: even at vanishingly low microwave powers $P_{\text{micr}} \approx 10^{-7} - 10^{-8}$ W the profile of the absorption lines in this spectrum had the form of a distorted dispersion curve and varied with the orientations of \mathbf{H}_0 and \mathbf{E}_1 . One should point out that these features were not associated with passage relaxation effects. This was deduced from an analysis of the data in Fig. 3, and also from the results of direct measurements of the rate of spin relaxation of the center 2 by the method of pulse saturation, carried out using a superheterodyne spectrometer ($T_1 < 10^{-4}$ s at $T = 1.7$ K). This conclusion was supported by the observation that, for example, the characteristic profile of the lines shown in Fig. 2 and having the form of a distorted dispersion curve was retained practically without change in a wide range of temperatures (1.7–40 K) and powers P_{micr} ($10^{-5} - 10^{-8}$ W). The relaxation effects began to appear at $T = 4.2$ K at powers $P_{\text{micr}} \gtrsim 10^{-4}$ W (see Fig. 3), which resulted in an additional characteristic change in the nature of the spin resonance spectra of the centers 2 and 3 (Fig. 4).

It was found that the presence of the centers 2 and 3 was correlated with the appearance of a considerable microwave conductivity of the samples, deduced from a strong reduction in the Q factor of the working resonator. The microwave conductivity did not fall when T dropped all the way down to 1.7 K, but was accompanied by the appearance of acceptor levels in the band gap of silicon (these levels were detected in electrical measurements and from the results of an ESR study in the presence of illumination).

Interband illumination ($h\nu \approx 1$ eV) at $T \lesssim 15$ K destroyed the spin resonance spectra of the centers 2 and 3 and the microwave conductivity, and the Q factor became close to the Q factor of the loaded resonator. When illumination was switched off, the spin resonance spectra and the microwave conductivity were restored after a time which decreased as the temperature and the concentration of the uncompensated shallow TD-II donors in the samples increased. For example, in the samples with the boron concentration in the range $\gtrsim 10^{15}$ cm $^{-3}$ it was found that there was no significant recovery up to ~ 1 h at $T \lesssim 4.2$ K. On the other hand, in the case of the original n -type Si samples, characterized by a considerable concentration of the uncompensated shallow TD-II donors, it was found that the spin resonance signals and microwave conductivity were partly restored after 20 s at $T = 4.2$ K and at $T \approx 20$ K the intensi-

ties of the spin resonance signals emitted by these samples were practically unaffected by the interband illumination. When the illumination took place across a germanium filter ($h\nu \leq 0.66$ eV), the spin resonance spectra and the microwave conductivity were not affected, but the recovery time of the spin resonance signals and the microwave conductivity shortened after the end of the interband illumination. An increase in temperature caused a gradual reduction in the intensities of the spin resonance lines of the centers 2 and 3.

The microwave conductivity and the spin resonance of the centers 2 and 3 were destroyed by annealing the samples at $T \gtrsim 1100$ K and also by electron ($E = 1.5$ MeV) or γ irradiation (from a ^{60}Co source). Prolonged application (~ 1 h) of ultrasound ($f \approx 1$ MHz) had the following effects on the concentrations of the centers 2 and 3 and on the microwave conductivity: at low ultrasound amplitudes there were no effects; when the amplitude reached a certain threshold value, the microwave conductivity and the concentration of the centers increased considerably; the subsequent annealing at $T \approx 920 - 1020$ K for 1–10 h also increased these parameters. Further increase in the amplitude of ultrasound destroyed the microwave conductivity and the spin resonance of the 2 and 3 centers.

It should be pointed out that, in addition to these spectra of the centers 2 and 3, the same samples exhibited also a series of weak lines of similar nature, which we could not identify because of their overlap with the stronger lines of the investigated centers.

4. THEORY AND DISCUSSION

a) Value of the g tensor

All the observed resonance lines were due to paramagnetic centers with the spin $S = 1/2$. The spin Hamiltonian of these centers in a coordinate system linked to the directions of the principal axes of the g tensor (l_i, m_i, n_i) can be described by

$$\mathcal{H} = \sum_i g_i \beta S_i H_i, \quad i=1, 2, 3. \quad (1)$$

Diagonalization of the Hamiltonian (1) yields the following expression for the g tensor as a function of the Euler angles of the field \mathbf{H}_0 :

$$g^2 = \frac{1}{2} \sum_{i=1}^3 g_i^2 [n_i^2 + (l_i \cos \varphi + m_i \sin \varphi)^2] + \frac{1}{2} \cos 2\theta \sum_{i=1}^3 g_i^2 [n_i^2 - (l_i \cos \varphi + m_i \sin \varphi)^2] + \sin 2\theta \sum_{i=1}^3 g_i^2 n_i (l_i \cos \varphi + m_i \sin \varphi). \quad (2)$$

Using Eq. (2), we describe the experimental data of Fig. 1 by the parameters of the g tensors of three types of center, listed in Table I. All the centers had the local C_s symmetry. The parameters of the center 2 agreed, to within the limits of the experimental error, with the parameters of one of the centers discussed in Ref. 15, whereas the parameters of the center 3 differed from those of the second center considered in Ref. 15. Bearing in mind the complexity and variability of the spectra of different samples and the influence of the condi-

TABLE I. Principal values and direction cosines of main axes of the g tensors of the Si-2K, Si-3K, and Si-4K centers.

	g_1	g_2	g_3	1	2	3
Si-2K	1.9982	2.0014	1.9930	$\langle \frac{1}{\sqrt{2}}, -\frac{1}{\sqrt{2}}, 0 \rangle$	$\langle \frac{n_2}{\sqrt{2}}, \frac{n_1}{\sqrt{2}}, n_3 \rangle$	$\langle -\frac{n_2}{\sqrt{2}}, -\frac{n_1}{\sqrt{2}}, n_3 \rangle$
Si-3K	1.9994	2.0018	1.9920	$\langle \frac{1}{\sqrt{2}}, -\frac{1}{\sqrt{2}}, 0 \rangle$	$\langle \frac{n_2'}{\sqrt{2}}, \frac{n_1'}{\sqrt{2}}, n_3' \rangle$	$\langle -\frac{n_2'}{\sqrt{2}}, -\frac{n_1'}{\sqrt{2}}, n_3' \rangle$
Si-4K	1.9962	2.0002	1.9920	$\langle 0, 1, 0 \rangle$	$\langle \frac{1}{\sqrt{2}}, 0, \frac{1}{\sqrt{2}} \rangle$	$\langle -\frac{1}{\sqrt{2}}, 0, \frac{1}{\sqrt{2}} \rangle$

*Here, $n_2 = 0.924$, $n_2' = 0.946$, $n_3 = 0.383$, and $n_3' = 0.326$. The values of the g factor are given to within $\pm 2 \times 10^{-4}$.

tions during recording of the spectra, we assigned the spectral lines to specific centers using both the experimental data of Fig. 1 and additional factors such as the behavior of the spectrum on deviation from a crystallographic plane by a small angle, the dependences of the line intensities on the orientation of \mathbf{E}_1 , and the difference in the behavior of the intensities of different lines (particularly lines 1, 2, and 3–6 in Fig. 1a).

The directions of the principal axes of the g tensor of the center 2 were found to be parallel to the $\mathbf{l} \parallel \langle 110 \rangle$ dislocation axis, as well as to the vector \mathbf{d} lying in the plane of a dislocation dipole $\mathbf{d} \parallel \mathbf{l}$ and the normal to this plane $\mathbf{h} \parallel [113]$. Such dislocation dipoles consisting of two 60° partial dislocations with antiparallel Burgers vectors were found in Ref. 16 by electron microscopy for silicon samples subjected to the same heat treatment. One of the principal axes of the g tensors of the centers 2 and 3 was close in direction to the $[113]$ crystallographic axis, but the angle between the 2 axis and the $[001]$ direction was 23° for the center 2 and 19° for the center 3. The presence of the center 3 had a tendency to rotate the plane of the dislocation dipole from (113) to (001) , as reported in Ref. 16.

We found that, in addition to the 60° dislocations, our silicon samples contained also 90° dislocations, which formed dipoles with the (001) plane. The Si-4K centers (Table I) located at these dipoles should have spectral lines in the (110) plane coinciding with the lines 3–5 in Fig. 1a. Their presence was possibly indicated by the high intensity of these lines. On the other hand, in the (001) plane these centers should give rise to two lines with angular dependence $g = 1.9962 \pm 0.0042 \sin 2\theta$ and one line independent of the orientation of \mathbf{H}_0 with $g = 1.9962$. We did not observe the first pair of lines, but its existence could be found on the basis of Fig. 3 in Ref. 15, where at $\theta = 45^\circ$ there were points with $g = 2.0004$ and 1.9920 not identified in Ref. 15.

We thus concluded that all the observed spin resonance lines were due to paramagnetic centers which were built into the dislocation cores forming a dislocation dipole. For this reason the symmetry of the centers 2, 3, and 4 was not axial but C_s . The principal axes of the g tensors coincided with special axes of the dislocation dipoles. The dependence of the spin resonance signal on \mathbf{E}_1 should prove this hypothesis.

b) Electric-dipole spin resonance

The dependence of the intensities of the spin resonance signals of the centers 2 and 3 on the intensity and the direction of \mathbf{E}_1 and the nature of their saturation indicated that the spectrum was due to transitions, induced by an electric field, between the spin sublevels of the local centers, i.e., due

to an electric-dipole spin resonance (EDSR).^{13,17} The proximity of the g components to 2 and $S = 1/2$ demonstrate that the EDSR occurred at an electron center.

The mechanisms of the EDSR proposed for shallow donors in Refs. 13 and 17 give rise to a dependence of the intensity of the EDSR signals on H_0 , proportional to H_0^3 . Our experiment at $\nu_{\text{micr}} \approx 35$ GHz demonstrated only the usual dependence on H_0 (which was proportional to $g\beta H_0/kT$, where β is the Bohr magneton) related to the difference between the populations of the Kramers doublet.

If in the initial Hamiltonian of Eq. (10) in Ref. 17 we replace the operator of the donor–donor interaction $e\mathbf{E}\cdot\mathbf{r}$ with a more effective (in our case) operator representing the interaction of a donor electron with the elastic deformation potential of a dislocation dipole $V(\mathbf{r})$ and if we include also the operator \mathcal{H}_{so} representing the spin–orbit interaction between the donor electron spin and the orbital motion in the potential of the dislocations, we find that a matrix element for an induced transition between the Kramers-conjugate states appears in the second order of perturbation theory with respect to $V(\mathbf{r})$ and \mathcal{H}_{so} , in contrast to Ref. 17, where we need the third order of perturbation theory in respect of $e\mathbf{E}\cdot\mathbf{r}$ and $g\beta\mathbf{H}_0\cdot\mathbf{S}$. The Hamiltonian of the donors is in the form

$$\mathcal{H} = \mathcal{H}_0 + \mathcal{H}_1 + \mathcal{H}'(t), \quad (3)$$

where \mathcal{H}_0 is the unperturbed Hamiltonian of the donor governing the unperturbed states A , T , and E of the donor in silicon and their Zeeman splitting in the $1s$ multiplet of the donor

$$\mathcal{H}_1 = V(\mathbf{r}) + \mathcal{H}_{\text{so}}^{(0)}, \quad \mathcal{H}_{\text{so}}^{(0)} = \frac{\hbar^2}{m^2 c^2} [\nabla V(\mathbf{r}), \mathbf{k}_0] \mathbf{S}, \quad (3a)$$

\mathbf{k}_0 is the quasimomentum of an electron at a minimum of the conduction band, and

$$\mathcal{H}'(t) = e\mathbf{E}_1 \mathbf{r} + \frac{\hbar}{m^2 c^2} \left[\nabla V(\mathbf{r}), \frac{e}{c} \mathbf{A} \right] \mathbf{S} = e\mathbf{E}_1 \mathbf{r} + \mathcal{H}_{\text{so}}^{(1)} \quad (3b)$$

is a time-dependent operator of the perturbation which is responsible for the induced transitions. The matrix element of the induced electric-dipole transition obtained in second order of perturbation theory using the operators (3a) and (3b) between the spin sublevels of the ground state of a donor A_σ and $A_{\sigma'}$ (σ and σ' are the spin projections) is

$$\langle A_\sigma | \mathcal{H}_1 + \mathcal{H}'(t) | A_{\sigma'} \rangle = W_{1\sigma\sigma'} + W_{2\sigma\sigma'}, \quad (4)$$

$$W_{1\sigma\sigma'} = \sum_i \frac{\langle A_\sigma | e\mathbf{E}_1 \mathbf{r} | \Psi_{i\sigma} \rangle \langle \Psi_{i\sigma} | \mathcal{H}_{\text{so}}^{(0)} | A_{\sigma'} \rangle}{E_A - E_i}, \quad (4a)$$

$$W_{2\sigma\sigma'} = \sum_i \frac{\langle A_\sigma | V(\mathbf{r}) | \psi_{i\sigma} \rangle \langle \psi_{i\sigma} | \mathcal{H}_{so}^{(1)} | A_{\sigma'} \rangle}{E_A - E_i}, \quad (4b)$$

where E_A and E_i ($i = T, E$) are the energies of the 1s multiplet of a donor in silicon in the A , T , and E states. An estimate shows that $W_{2\sigma\sigma'}$ is approximately two orders of magnitude higher than $W_{1\sigma\sigma'}$, if both differ from zero. However, $W_{2\sigma\sigma'} \neq 0$ only if the operators $V(\mathbf{r})$ and $\nabla V(\mathbf{r})$ have the same parity.

The elastic deformation potential near dislocations can be found in terms of components of the stress tensor:

$$V(\mathbf{r}) = \sum_{i,j} \lambda_{ij} \sigma_{ij}(r)$$

$[\sigma_{ij}(r)]$ is the stress tensor and λ_{ij} is the strain tensor]. The stress tensor near a dislocation in silicon is given by¹⁸

$$\begin{aligned} \sigma_{bb} &= -D \frac{r_h(2r^2 + r_b^2 - r_h^2)}{r^4}, & \sigma_{hh} &= D \frac{r_h(r_b^2 - r_h^2)}{r^4}, \\ \sigma_{il} &= \nu(\sigma_{bb} + \sigma_{hh}), \\ \sigma_{bh} &= \sigma_{hb} = D \frac{r_b(r_b^2 - r_h^2)}{r^4}, & D &= \mu b / 2\pi(1 - \nu_p). \end{aligned} \quad (5)$$

The following notation is used in the system of equations (5): $b = 3.84 \text{ \AA}$ is the length of the Burgers vector; ν_p is the Poisson ratio; $\mu = 7.55 \times 10^{11} \text{ dyn/cm}^2$ is the shear modulus; r_b and r_h are the projections of \mathbf{r} along the \mathbf{b} and \mathbf{h} axes (\mathbf{b} , \mathbf{l} , and \mathbf{h} are unit vectors along the Burgers vector, dislocation axis, and normal to their plane). We can see from Eq. (5) that all σ_{ij} and, consequently, V are odd functions of r so that the components of ∇V_{ij} are even. In this case only the matrix element $W_{1\sigma\sigma'}$ in Eq. (4) differs from zero. Such a situation applies to centers at free dislocations.

When dislocations form dipoles, the stress tensor is equal to the difference between the tensors of Eq. (5) for two coupled dislocations.

$$\sigma_{ii}' = \sigma_{ii}(|\mathbf{r}|) - \sigma_{ii}(|\mathbf{r} + \mathbf{d}|). \quad (6)$$

When Eq. (6) is expanded as a series in $(|\mathbf{r}|/|\mathbf{d}|)$, the components of the tensor σ_{ii}' contain terms of different parity. As a result, V_{ij} and ΔV_{ij} contain terms of the same parity and Eq. (4) is dominated by $W_{2\sigma\sigma'}$ which is so much larger than $W_{1\sigma\sigma'}$ that the latter can be ignored.

It therefore follows that for the centers 2 and 3 the induced transitions in the EDSR are determined by the matrix element $W_{2\sigma\sigma'}$ where $V(\mathbf{r})$ and $\nabla V(\mathbf{r})$ are calculated using Eqs. (5) and (6).

Averaging the matrix element $W_{2\sigma\sigma'}$ over the spatial coordinates, we shall supplement the spin Hamiltonian of Eq. (1) of an electron at a dislocation dipole by a perturbation operator which is a function of time:

$$\begin{aligned} \mathcal{H} &= \omega_0 S_z + [h_1(\theta, \varphi, \theta_1) S_x + h_2(\theta, \varphi, \theta_1) S_y] \cos \omega t, \\ \omega_0 &= g\beta H_0, & h_1(\theta, \varphi, \theta_1) &= \lambda[\mathbf{e}\mathbf{q}]_x, & h_2(\theta, \varphi, \theta_1) &= \lambda[\mathbf{e}\mathbf{q}]_y, \\ \lambda &= \frac{e\mathbf{E}_1}{m^2 c^2 \omega} \sum_i \frac{\langle A | \nabla V | \psi_i \rangle \langle \psi_i | V | A \rangle}{E_A - E_i}. \end{aligned} \quad (7)$$

The following notation is used in the system (7): $\mathbf{e} \parallel \mathbf{E}_1, \mathbf{q} \parallel \nabla V, |\mathbf{e}| = 1, |\mathbf{q}| = 1$; the Hamiltonian \mathcal{H} is written

down in a coordinate system attached to a static magnetic field $\mathbf{H}_0 \parallel \mathbf{z}$; θ and φ are the Euler angles of \mathbf{H}_0 ; $\theta_1 = \mathbf{E}_1 \mathbf{z}$; ψ_i are the wave functions of excited states of the 1s multiplet of a donor in silicon.

The absorption of microwave power in a conducting sample is determined by the surface impedance of a sample (or a dislocation dipole in the present case):

$$P = \left(\frac{c}{4\pi}\right)^2 H_{10}^2 \text{Re } Z, \quad Z = \frac{4\pi \mathbf{n}[\mathbf{E}_{10}\mathbf{H}_{10}]}{c H_{10}^2}, \quad (8)$$

where \mathbf{E}_{10} and \mathbf{H}_{10} are the values of the fields on that surface of the sample which is perpendicular to the propagation vector of the microwave field. Using the condition of continuity of the tangential components of $\mathbf{H}_{1\perp}$ and of the magnetic induction $\mathbf{B}_1 = \mathbf{H}_{1\perp} + 4\pi\mathbf{M}_1$ (\mathbf{M}_1 is the tangential component of the magnetization), we find that under spin resonance conditions the absorption of microwave power is equal to the change in the impedance Z :

$$Z = Z_0 \left[1 + \frac{4\pi}{H_{10}^2} \overline{\mathbf{M}_1(t) \mathbf{H}_{1x}(t)} \right], \quad (9)$$

where

$$\overline{M_x(t)} = M_{\perp}(t) = \frac{1}{2} [\rho_{12}(t) + \rho_{21}(t)].$$

The bar in Eq. (9) denotes averaging with respect to time; Z_0 is the impedance far from a resonance; ρ_{mn} are the components of the spin density matrix. Using the familiar heat equations for a spin density matrix

$$\begin{aligned} \dot{\rho}_{mn} &= i[\mathcal{H}, \rho]_{mn} - (\rho_{mn} - \rho_{mn}^{(0)}) T_{mn}^{-1}, \\ T_{mn}^{-1} &= \begin{cases} T_1^{-1}, & m=n \\ T_2^{-1}, & m \neq n \end{cases} \end{aligned}$$

where T_2 is the relaxation time of the transverse magnetization, we can easily show that the profile of a signal representing $v = \chi'' h_0 = P/h_0$ is of the following form:

$$v = -\chi_0 \omega T_2 h_0 \frac{\sin \Phi - \Delta T_2 \cos \Phi}{1 + \Delta^2 T_2^2 + 4h_0^2 T_1 T_2}, \quad (10)$$

where

$$h_0 = (h_1^2 + h_2^2)^{1/2}, \quad \Phi = \sin^{-1}(h_2/h_0), \quad \Delta = \omega - \omega_0.$$

The solution (10) represents an inverted (compared with the usual ESR) asymmetric line. The profile and the intensity of this signal are described by the functions $h_1(\theta, \varphi, \theta_1)$ and $h_2(\theta, \varphi, \theta_1)$, which—according to Eq. (7)—depend on the value of λ and on the mutual orientation of the three vectors \mathbf{H}_0 , \mathbf{E}_1 , and ∇V . An estimate shows that the amplitude of the signal (10) is almost two orders of magnitude greater than the amplitude of the ordinary ESR signal.

The angular dependences of h_1 and h_2 are given by the following expressions:

$$\begin{aligned} h_1(\theta, \theta_1) &= \lambda \{ \sin \theta_E (g_h n_h + g_b n_b) \\ &\quad - \cos \theta_E [(l_h + m_h) g_h + g_b (l_b + m_b)] \}, \\ h_2(\theta, \theta_1) &= \lambda \cos(\theta - \theta_E) [(l_h - m_h) g_h + g_b (l_b - m_b)]. \end{aligned} \quad (11)$$

Here, l_{bj} , m_{bh} , and n_{bh} are the direction cosines of the Burgers vector and of the normal vector, measured relative to the crystallographic axes. The system (11) is derived assuming, for the sake of simplicity, that \mathbf{E}_1 and \mathbf{H}_0 rotate in the (110) plane; θ_E and θ are the polar angles of \mathbf{E}_1 and \mathbf{H}_0

relative to the [001] axis. The constants g_h and g_b are proportional to the projections of the vector ∇V along the \mathbf{h} and \mathbf{b} axes, i.e., they are governed by the distribution of the gradient of the elastic potential of a dislocation dipole in a plane perpendicular to \mathbf{l} . Equations (5) and (6) yield $g_h \approx 0.3$ and $g_b \approx 0.9$ for a dislocation dipole.

We shall assume the profile function of Eq. (10) and find the positions of extrema $\Delta_1 T_2$ and $\Delta_2 T_2$ as well as extremal values $v(\Delta_1 T_2)$ and $v(\Delta_2 T_2)$. Then, the amplitude of the signal is $I = v(\Delta_1 T_2) - v(\Delta_2 T_2)$. We find that

$$I = -\chi_0 \omega T_2 [h_1^2(\theta, \theta_E) + h_2^2(\theta, \theta_E)]^{1/2}, \quad (12)$$

and using Eq. (11), we obtain the dependence of the amplitude of the observed signals on the orientation of the electric component of the microwave field in the case when $\theta = 0$ ($\mathbf{H}_0 \parallel [001]$).

$$I(\theta=0) \propto \{n^2 + 1/2(l_+^2 + l_-^2) - \cos 2\theta_E [n^2 - 1/2(l_+^2 - l_-^2)] - \sqrt{2}nl_+ \sin 2\theta_E\}, \quad (13)$$

$$n = n_h + 2.5n_b, \quad l_+ = (l_h + m_h) + 2.5(l_b + m_b),$$

$$l_- = (l_h - m_h) + 2.5(l_b - m_b).$$

It is clear from Eq. (13) that the dependence of the intensities of the EDSR signals on the orientation of \mathbf{E}_1 is governed by the directions of the Burgers vector \mathbf{b} , of the dislocation axis \mathbf{l} , and of the normal to their plane. If we bear in mind that in the case of dislocations with axes of the [110] type the Burgers vectors are directed along axes of the $[\bar{1}, 1, 2]$ type, so that $\mathbf{h} \perp [1, \bar{1}, 1]$, we obtain four types of $I(\theta = 0, \theta_E)$ curves:

$$I_1(\theta_E) \propto \sin^2 \theta_E, \quad I_2(\theta_E) \propto \cos^2 \theta_E + 0.13 \sin 2\theta_E,$$

$$I_{3,4}(\theta_E) \propto 1 + 0.41 \cos 2\theta_E \pm 0.91 \sin 2\theta_E,$$

which are shown in Fig. 5. We can see that the theoretical results are in satisfactory agreement with the experimental data.

The observed profile of the EDSR lines is also described well by Eq. (10) (see Fig. 6 and also Figs. 2 and 4). The fact that an increase in the microwave power increases the degree

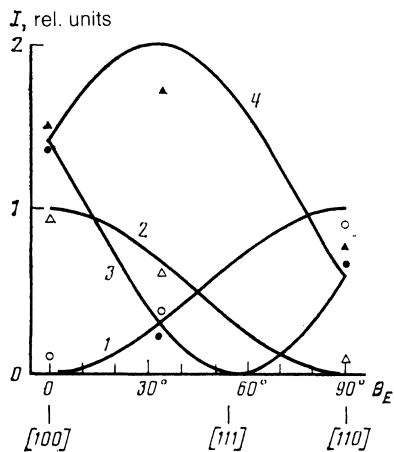


FIG. 5. Dependences of the intensities of the EDSR lines of the Si-2K centers on the orientation of \mathbf{E}_1 in the case when $\mathbf{H}_0 \parallel [100]$; the continuous curves are theoretical and the points are the experimental results: \circ) lines 1, 2, and 5 (Fig. 1); Δ) line 4; \blacktriangle) line 6; \bullet) line 3. The experimental points were recorded for $\theta = 10^\circ$.

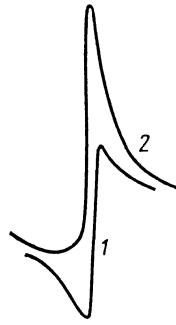


FIG. 6. Calculated profile of the EDSR line of the Si-2K centers in the case when $\mathbf{E}_1 \parallel [100]$: 1) $\mathbf{H}_0 \parallel [\bar{1}\bar{1}1]$; 2) $\mathbf{H}_0 \parallel [111]$.

of asymmetry of the individual lines (Fig. 4) is easily understood from Eq. (10) if we compare the profile of the signal in the absence of saturation with the profile of the saturated EDSR signal. In the case of strong saturation the widths of the individual lines increase tending to the limit $2h_0 T_1^{1/2}$, the lines then overlap forming a single envelope, but the profile of this envelope still retains the characteristic form of an asymmetric dispersion signal.

c) Discussion of results

All our experimental observations can be explained if we assume that the microwave conductivity of our samples and the EDSR spectra of the Si-2K and Si-3K centers are due to the presence of rod- and ribbon-shaped stacking faults.^{10,19} Such defects are characterized by dislocation dipoles in the (113) and (100) planes,^{15,19} coinciding in direction with the principal axis of the g tensor of the centers 2 and 3. These dislocation dipoles may be responsible for the microwave conductivity.^{5,7} Since the dipoles are connected by short conducting segments in a low-conductivity (at low temperatures) crystal matrix, the dc conductivity of such samples is low. The rod- and ribbon-shaped defects and the associated dislocation dipoles are transformed into other defects (the dislocation dipoles become perfect dislocation loops) as a result of high-temperature annealing ($T_{\text{ann}} \approx 1120$ K) following electron irradiation.¹⁹ The suppression of the microwave conductivity and the EDSR of the centers 2 and 3 we observed after such treatments and also after γ -ray irradiation indicates a similar transformation of the defects occurring in our samples.

The influence of ultrasound further confirms the dislocation origin of our centers. In fact, the threshold effect of ultrasonic vibrations can be explained by detachment of dislocation dipoles from point obstacles and their further motion, which increases the effective concentration of the paramagnetic centers. Suppression of the microwave conductivity state and of the centers 2, 3, and 4 can be explained by transformation of dislocation dipoles into perfect loops.

The paramagnetic centers 2, 3, and 4 are built into dislocation cores which represent dislocation dipoles, so that they have a low symmetry C_s . The crystal potential due to these dislocation dipoles allows electric-dipole microwave transitions. The EDSR explains our experimental results (including the profiles of the observed lines, the angular dependences of the line intensities I , and the dependence of I on the \mathbf{E}_1 component of the microwave field).

In the case of interband illumination the dislocation dipoles capture holes which recombine with electrons and suppress the microwave conductivity. The charge exchange also makes the centers 2, 3, and 4 nonparamagnetic and the electric-dipole spin resonance is no longer observed. Recovery of the microwave conductivity and of the EDSR signals after the end of interband illumination is due to thermal ionization of electrons which are released from the shallow TD-II levels (filled with electrons as a result of illumination, which increases the ESR signal of TD-II) and this is followed by subsequent capture by dislocation levels.

There is an analogy between the properties of the centers 2 and 3 in our undeformed samples and the properties of Ch centers⁸ found in silicon samples deformed plastically at $T = 950$ K. This is the dependence of the spin resonance signals on the E_1 component of the microwave field and observation of an inverted asymmetric resonance line. However, differences in the response to optical illumination as well as differences in the principal values of the g tensor and in the sign of the photocorrection to the microwave conductivity indicate that the Si-2K, Si-3K, and Ch centers are different.

It seems very probable that in our case the formation of ribbon- and rod-shaped defects is due to precipitates of oxygen atoms (resulting in the formation of the TD-II centers). When a certain critical size is reached, these precipitates are accompanied by dislocation dipoles containing the centers 2 and 3. This is confirmed by the following observations: 1) in samples with high carbon concentrations, where large precipitates and the corresponding deep TD-II centers do not form,¹¹ there are no centers 2, 3, and 4; 2) high-temperature annealing ($T_{\text{ann}} \approx 1170$ K) destroys simultaneously the deep TD-II centers as well as the centers 2, 3, and 4.

We have thus investigated a new class of centers of dislocation origin, which appear in undeformed heat-treated silicon with a high oxygen concentration. A theory of an

electric-dipole spin resonance is developed and it explains satisfactorily the experimental results.

- ¹V. A. Grazhulis, V. V. Kveder, V. Yu. Mukhina, and Yu. A. Osip'yan, *Pis'ma Zh. Eksp. Teor. Fiz.* **24**, 164 (1976) [*JETP Lett.* **24**, 142 (1976)].
- ²V. A. Grazhulis and Yu. A. Osip'yan, *Zh. Eksp. Teor. Fiz.* **60**, 1150 (1971) (*Sov. Phys. JETP* **33**, 623 (1971)).
- ³T. Wosinski, T. Figielski, and A. Makosa, *Phys. Status Solidi A* **37**, K57 (1976).
- ⁴V. V. Kveder and Yu. A. Osip'yan, *Zh. Eksp. Teor. Fiz.* **80**, 1206 (1981) [*Sov. Phys. JETP* **53**, 618 (1981)].
- ⁵V. V. Kveder, Yu. A. Osip'yan, and A. I. Shalynin, *Zh. Eksp. Teor. Fiz.* **88**, 309 (1985) (*Sov. Phys. JETP* **61**, 182 (1985)).
- ⁶V. V. Kveder, Yu. A. Osip'yan, and A. I. Shalynin, *Pis'ma Zh. Eksp. Teor. Fiz.* **40**, 10 (1984) [*JETP Lett.* **40**, 729 (1984)].
- ⁷V. V. Kveder, Yu. A. Osip'yan, I. R. Sagdeev, A. I. Shalynin, and M. N. Zolotukhin, *Phys. Status Solidi A* **87**, 657 (1985).
- ⁸V. V. Kveder, V. Ya. Kravchenko, T. R. Mchedlidze, Yu. A. Osip'yan, D. E. Khmel'nitskii, and A. I. Shalynin, *Pis'ma Zh. Eksp. Teor. Fiz.* **43**, 202 (1986) [*JETP Lett.* **43**, 255 (1986)].
- ⁹H. Alexander, C. Kisielowski-Kemmerich, and E. R. Weber, *Physica B (Utrecht)* **116**, 583 (1983).
- ¹⁰A. Bourett, *Proc. Thirteenth Intern. Conf. on Defects in Semiconductors*, Coronado, CA, 1984, publ. by Metallurgical Society of AIME, Warrendale, PA (1985), p. 129.
- ¹¹V. M. Babich, N. P. Baran, A. A. Bugai, *et al.*, Deposited Paper No. R4619 [in Russian], VINITI, Moscow (1987).
- ¹²V. M. Babich, N. P. Baran, A. A. Bugai, A. A. Konchits, and V. M. Maksimenko, *Pis'ma Zh. Eksp. Teor. Fiz.* **44**, 513 (1986) [*JETP Lett.* **44**, 660 (1986)].
- ¹³É. I. Rashba and V. I. Sheka, *Fiz. Tverd. Tela (Leningrad)* **6**, 141 (1964) [*Sov. Phys. Solid State* **6**, 114 (1964)].
- ¹⁴V. L. Bonch-Bruевич, I. P. Zvyagin, R. Keiper, A. G. Mironov, R. Enderlein, and B. Esser, *Electronic Theory of Disordered Semiconductors* [in Russian], Nauka, Moscow (1981), p. 180.
- ¹⁵R. Wörner and O. F. Schirmer, *Phys. Rev. B* **34**, 1381 (1986).
- ¹⁶H. Bender, *Phys. Status Solidi A* **86**, 245 (1984).
- ¹⁷V. I. Mel'nikov and É. I. Rashba, *Zh. Eksp. Teor. Fiz.* **61**, 2530 (1971) [*Sov. Phys. JETP* **34**, 1353 (1972)].
- ¹⁸J. Friedel, *Dislocations*, Pergamon Press, Oxford (1964).
- ¹⁹H. Bartsch, J. Heidenreich, D. Hochl, and P. Werner, Abstracts of Papers presented at Fifth Intern. Conf. on Properties and Structure of Dislocations in Semiconductors, Moscow, 1986 [in Russian], p. 39.

Translated by A. Tybulewicz